Adsorption of Cu^{2+} to biomass ash and its modified product

Lei Xu, Hongbiao Cui, Xuebo Zheng, Jiani Liang, Xiangyu Xing, Lunguang Yao, Zhaojin Chen and Jing Zhou

ABSTRACT

Ash produced by biomass power plants has great potential for the removal of heavy metal ions from aqueous solution. The pollution of toxic heavy metals to water is a worldwide environmental problem. Discharges containing copper, in particular, are strictly controlled because the excessive copper can cause serious harm to the environment and human health. This work aims to investigate the adsorption characteristics of copper ions in aqueous solution by biomass ash and the modified products, and to evaluate their potential application in water pollution control. The biomass ash was modified with a mesoporous siliceous material and functionalized with 3-aminopropyltriethoxysilane. The surface properties of the biomass ash and the new matrix were studied to evaluate their adsorption property for Cu^{2+} ions at different pHs, initial metal concentrations and the thermodynamic and kinetic were studied. The chemical and morphological properties of this modified material are analyzed; the specific surface area of the modified biomass ash was nine times that of the initial ash. Both of the two materials showed a strong affinity for Cu^{2+}, and the Langmuir model could best represent the adsorption characteristics of Cu^{2+} on the two kinds of materials. The adsorption capacity of copper on the material increased with the increase of pH and pH 6 was the optimum pH. Thermodynamic analysis results showed that the adsorption of Cu^{2+} was spontaneous and endothermic in nature. The adsorptions of Cu^{2+} onto the modified biomass ash followed pseudo-second-order kinetics.

Key words | adsorption, biomass ash, copper, modification, nanomaterials

Lei Xu
Jiani Liang
Jing Zhou (corresponding author)
Key Laboratory of Soil Environment and Pollution Remediation,
Institute of Soil Science, Chinese Academy of Science,
Nanjing 210008, China
E-mail: zhoujing@issas.ac.cn

Lei Xu
College of Environmental Science and Tourism,
Nanyang Normal University,
Nanyang 473061, China

Lei Xu
Lunguang Yao
Zhaojin Chen
Collaborative Innovation Center of Water Security for Water Source Region of Mid-line of South-to-North Diversion Project of Henan Province,
Nanyang Normal University,
Nanyang 473061, China

Hongbiao Cui
School of Earth and Environment,
Anhui University of Science and Technology,
Huainan 232001, China

Xuebo Zheng
Shandong Industrial Engineering Laboratory of Biogas Production & Utilization, Key Laboratory of Biofuels,
Qingdao Institute of Bioenergy and Bioprocess Technology, Chinese Academy of Sciences,
Qingdao 266101, China

Xiangyu Xing
College of Non-Major Foreign Language Teaching,
Nanyang Normal University,
Nanyang 473061, China

Jing Zhou
Jiangxi Engineering Research Center of Eco-Remediation of Heavy Metal Pollution,
Jiangxi Academy of Science,
Nanchang 330096, China

INTRODUCTION

Generating electricity by combustion of biomass materials has become one of the strategies to solve the energy crisis for developed and developing countries. However, during the combustion, the inorganic constituents of the biomass form biomass ash, thus increasing its accumulation in the environment (Vamvuka & Kakaras 2011; Ciesielczuk et al. 2014). A large number of studies have been carried out on the accumulation of biomass ash, aiming to facilitate the potential industrial application (Williams 1997; James et al. 2012; Quirantes et al. 2016). Biomass ash shows good adsorption properties for metals; due to its plenty, it has been increasingly used as a cheap material for the removal of heavy metals from wastewater (Seweryn 2012; Okmanis et al. 2015). Compared with other technologies such as ion exchange, chemical

precipitation, electrochemical treatment, membrane technology, evaporation and solidification, the adsorption method has been widely used (Zhang *et al.* 2013). Massive mesoporous materials based on silicon dioxide have been extensively studied and partially commercialized (Xia & Mokaya 2003; Tamayo *et al.* 2015). These materials have many advantages such as a large specific surface area, good thermal and mechanical stability, homogenous pore and perfect pore morphology, high functionalization characteristics and high adsorption capacity (Krawiec & Kaskel 2006; Boukai *et al.* 2008). Furthermore, the adsorption capacity of these materials for some metal ions have been increased by combining some organic functionalities on the surface of the material and/or inside the pores (Messina & Schulz 2006; Saeung & Boonamnuayvitaya 2008; Alyoshina & Parfenyuk 2013). These materials with nanostructures can be used as an effective material for the removal of heavy metals from industrial waste water (Hao *et al.* 2016; Zhu *et al.* 2017), thus recovering valuable metals.

Heavy metals, especially copper (Cu), accumulate in the environment, causing serious threat to the environment and human health (Mendicino & Brown 1998; Ndilila *et al.* 2014; Takaishi *et al.* 2015). Studies show that Cu pollution has been a serious threat to food safety and human health in China (Hu *et al.* 2014; Wang *et al.* 2014). Many studies have reported the removal of Cu^{2+} from aqueous solutions, peanut shell, zeolite, coal fly ash, activated carbon, and biochar have been used to remove Cu^{2+} efficiently from aqueous solutions (Sočo & Kalembkiewicz 2013; Qiang *et al.* 2015; Demiral & Güngör 2016; Jiang *et al.* 2016; Shen *et al.* 2017); however, biomass ash, especially its modified product, have been rarely studied for Cu^{2+} adsorption. In this study, the efficiency of biomass ash, especially its modified product, for Cu^{2+} adsorption was investigated.

Herein, combining these two systems has the advantages of improvement of adsorption efficiency and the abundant availability in supply at no or low cost. Based on these premises, combined with these two cheap materials, developing a new material with stronger adsorption ability for Cu^{2+} and better stability in acidic medium was the main goal of this work. The strengthening and optimization of the conditions were emphasized in the process of the experiment.

MATERIALS AND METHODS

Biomass ash

The biomass ash sample was collected from a power plant firing agricultural residues in Anhui province, China.

Mixed feeds such as wheat stem, maize straw, groundnut shell, and cotton stalk were used in the power plant. They were fired in a traveling-grate furnace at ~850 °C with excess air. The ash was collected from the tank located below the grate. The elemental composition and morphology of the biomass ash were analyzed.

Modification experiment

The biomass ash was modified with a hexagonal mesoporous silica (HMS) matrix by co-condensation (Walcarius & Mercier 2010); the hexagonal structure changed after the reaction with biomass ash. Because of the presence of silicate, the modified hexagonal structure acted as a catalyst, increasing the reactivity of tetraethyl orthosilicate (TEOS). The synthesis was carried out as follows. First, 1.24 g dodecylamine was dissolved in an alcohol (10 mL), and then a mixture of 1.24 g biomass ash in 90 mL ultrapure water (CN61M-UPR-I-20 L) was added to it under stirring at 1,000 rpm. Then, 6.09 mL TEOS and 0.71 mL of an organosilane, 3-aminopropyltriethoxysilane (APS, NH$_2$(CH$_2$)3Si (OC$_2$H$_5$)$_3$), were added. After 30 s, 0.94 mL of trimethylbenzene (TMB) was added into the mixture, and then was stirred for 24 h. The mixture was then filtered through a 0.45 μm filter membrane and the remaining residue was air dried at room temperature. The remaining TMB was Soxhlet extracted with alcohol (125 mL) for 5 h. The sample was then air dried at room temperature for 24 h (Walcarius & Mercier 2010).

Physicochemical and morphological characterizations

The physicochemical properties of the biomass ash and modified biomass ash (modified with HMS matrix and functionalized with 10% APS) were evaluated by five analytical techniques. The elemental composition of the biomass ash was analyzed by inductively coupled plasma optical emission spectrometry (ICP-OES) (Perkin Elmer Optima 2000 optical emission spectrometer). The surface morphology of the biomass ash and modified biomass ash was observed using an S-4800 scanning electron microscope (SEM) (Hitachi, Tokyo, Japan) (Pizarro *et al.* 2015). Topographic analysis and quantification of the components of the biomass ash were performed using a JEM-2010HT transmission electron microscope (JEOL Ltd, Akishima, Tokyo, Japan) equipped with an energy-dispersive spectrometer (EDS). The functional groups present in the biomass ash were characterized by Fourier transform infrared spectroscopy (FTIR) using the Spectrum Two™ IR spectrometer (Perkin Elmer, Waltham, MA, USA)

in the range 4,000–500 cm^{-1} (Noli *et al.* 2015) and specific surface area was measured by the Brunauer–Emmett–Teller (BET) method (Pizarro *et al.* 2015).

Adsorption experiments

In order to evaluate the Cu^{2+} adsorption capacity of the modified material, various adsorption experiments were carried out. The effects of the initial Cu^{2+} concentration, pH, kinetic and thermodynamic were evaluated using guaranteed reagent. Copper solutions used in the experiment were prepared from copper standard solution of 1,000 mg/L $Cu(NO_3)_2$ in 0.5 M HNO_3 and ultrapure water (CN61M-UPR-I-20 L). The pH was adjusted with 0.1 M HNO_3 and 0.1 M NaOH.

Effect of pH

The effect of pH on the adsorption of metals can be attributed to the surface charge of the materials (biomass ash and modified biomass ash) and the distribution associated with the metal species (Cretescu *et al.* 2015). In order to determine the optimum pH, 0.1 g of the two adsorbents were respectively added to 25 mL solution with 50 mg/L Cu^{2+} in the pH range 2.0–8.0.

Adsorption equilibrium experiment

The adsorption capacity of the modified biomass ash was evaluated at different adsorbate concentrations by mixing 0.1 g of the adsorbent with 25 mL of a Cu^{2+} solution at the desired Cu^{2+} concentration (50–100 mg/L) adsorbate concentrations at initial pH 5. The adsorption experiments were carried out in 50 mL centrifuge tubes, under stirring at 150 rpm for 24 h, under the conditions of 30 °C. In order to study the thermodynamic characteristics of the adsorption process, the operating procedures were repeated at 45 and 60 °C.

Adsorption kinetics

The adsorption rate of the adsorbent in solution for metal ion can be understood by studying the kinetic characteristics of the adsorption process. Through the fitting of the experimental data with the kinetic model, the adsorption mechanism can be understood. The adsorption kinetics of Cu^{2+} was studied by adding 0.2 g of the modified biomass ash into the aqueous solution (100 mg/L, pH 5, 100 mL), and shaking with 150 rpm at 30 °C in a reciprocating

shaker, 5 mL sample was collected by pipette (Eppendorf, Research Plus, 0.5–5 mL) at 0.5, 1 , 2, 3, 5, 10, 15, 30, 60, 90, 120 180, 240 min, respectively. After equilibration, the suspension was centrifuged at 4,000 rpm for 10 min, then the supernatant was filtered with a 0.45 μm membrane, and the Cu^{2+} concentration in solution was determined by atomic absorption spectrophotometry (SpectrAA-220).

Data processing

Microsoft Excel 2010 (Microsoft Corp., Redmond, WA, USA) and SPSS 20.0 (IBM SPSS, Somers, NY, USA) were used to conduct the data processing.

RESULTS AND DISCUSSION

Physicochemical and morphological characteristics

The major elements present in the biomass ash were silicon, calcium, and potassium at concentrations of 120.40, 43.14, and 33.11 mg/g, respectively (Table 1). The SEM analysis results show that the biomass ash mainly consists of spherical particles and a part of sheet particles with diameters between 10 and 60 μm (Figure 1(a)), and the particles dispersed well. The results obtained for the modified biomass ash were markedly different from those obtained for the pure biomass ash with a clear spherical structure. The specific surface area of the modified biomass ash improved, and the surface was more smooth (Figure 1(b)). Moreover, some faint channels were observed, contributing to the improved porosity of the modified biomass ash.

The FTIR spectrum of the modified biomass ash (Figure 1(e)) demonstrates a intense absorption band at 3,330 cm^{-1}; this can be attributed to the O–H bonds of the silanol groups. The other absorption bands were observed at 850 cm^{-1} and 1,044 cm^{-1} which correspond to the symmetric and asymmetric Si–O–Si vibrations, respectively. After the functionalization of biomass ash with 10% (w/v) APS and HMS matrix, the spectrum was clearly different, showing a broad signal between 3,000 and 3,600 cm^{-1} which can be attributed to the improved number of silanol groups that exist in the synthesized material. The stretching bands can be attributed to the N–H group of APS, and the band at 1,488.2 cm^{-1} corresponds to the bending vibration of the N–H groups (Figure 1(e)) (Pizarro *et al.* 2015).

Table 2 shows the BET analyzes of the biomass ash and the modified material. The specific surface area of the modified material increased by >9 times compared with which of

Table 1 | Elemental composition of biomass ash analyzed by ICP-OES

Element	Si	Ca	K	Al	Fe	Mg	Na	P	S	Mn	Ni	Zn	Cu	Cr	Pb	Cd
Proportion (%)	12.04	4.31	3.31	2.11	1.08	0.65	0.42	0.41	0.073	0.034	0.018	0.015	0.0035	0.0022	0.0005	0.0002

the untreated biomass ash, from 21.38 ± 0.17 to 185.81 ± 0.15 m^2/g.

Figure 1(b) shows the size and structure of the synthesized materials, and Figure 1(d) shows the elemental composition of the two materials. The elemental composition shows the presence of C, O, Si, N, Al, Fe, and K. Both this analysis and FTIR analysis shows the presence of nitrogen which confirms the biomass ash has been functionalized by the primary amine (APS). Figure 1(b) shows the improved homogeneity of the surface of the modified biomass ash compared with the untreated biomass ash and some regular structure was formed; the specific surface area indicates that a functional mesoporous materials was obtained (Table 2).

Effect of pH

Studies on the use of adsorption in removing heavy metals from aqueous solutions indicate that pH is an important factor (Cao *et al.* 2016; Madani *et al.* 2017). The surface of biomass ash has a negative charge, which is transient and significantly depends on the pH of the solution (Cretescu *et al.* 2015). The adsorption of Cu^{2+} on the modified material was analyzed; Figure 2 shows the effects of different initial pH values on the load capacity (mg/g) for Cu^{2+} of the two materials. The Cu^{2+} adsorption was found to be highly pH-dependent. When pH was less than 4, both of the materials showed a very low adsorption capacity because of the competition between H$^+$ and Cu^{2+} for the active adsorption sites on the surface of the adsorbent (Liu *et al.* 2013), and the adsorption capacity increased sharply when the pH of the solution was increased (Ali *et al.* 2016).

When the pH in solution is very low, the number of H_3O^+ exceeded that of the metal ions by many times, and the material surface is almost completely covered by H_3O^+, which led to the reduction of adsorption capacity for metal ion (Gupta & Bhattacharyya 2008). When pH is gradually increasing, more and more H_3O^+ are removed from the material surface, thus making the metal ions can be close to the active adsorption sites on the material; this increases the binding of metal ions to the synthesized matrix surface through the mechanism of ion exchange (Gupta & Bhattacharyya 2008). When the pH >4, the H$^+$ concentration is greatly reduced, which is beneficial to the adsorption of metal ion on the surface of the material. This phenomenon can be attributed to the existence of oxides such as SiO_2, Fe_2O_3 and Al_2O_3 and their surface charge depends mainly on the pH in the solution. The
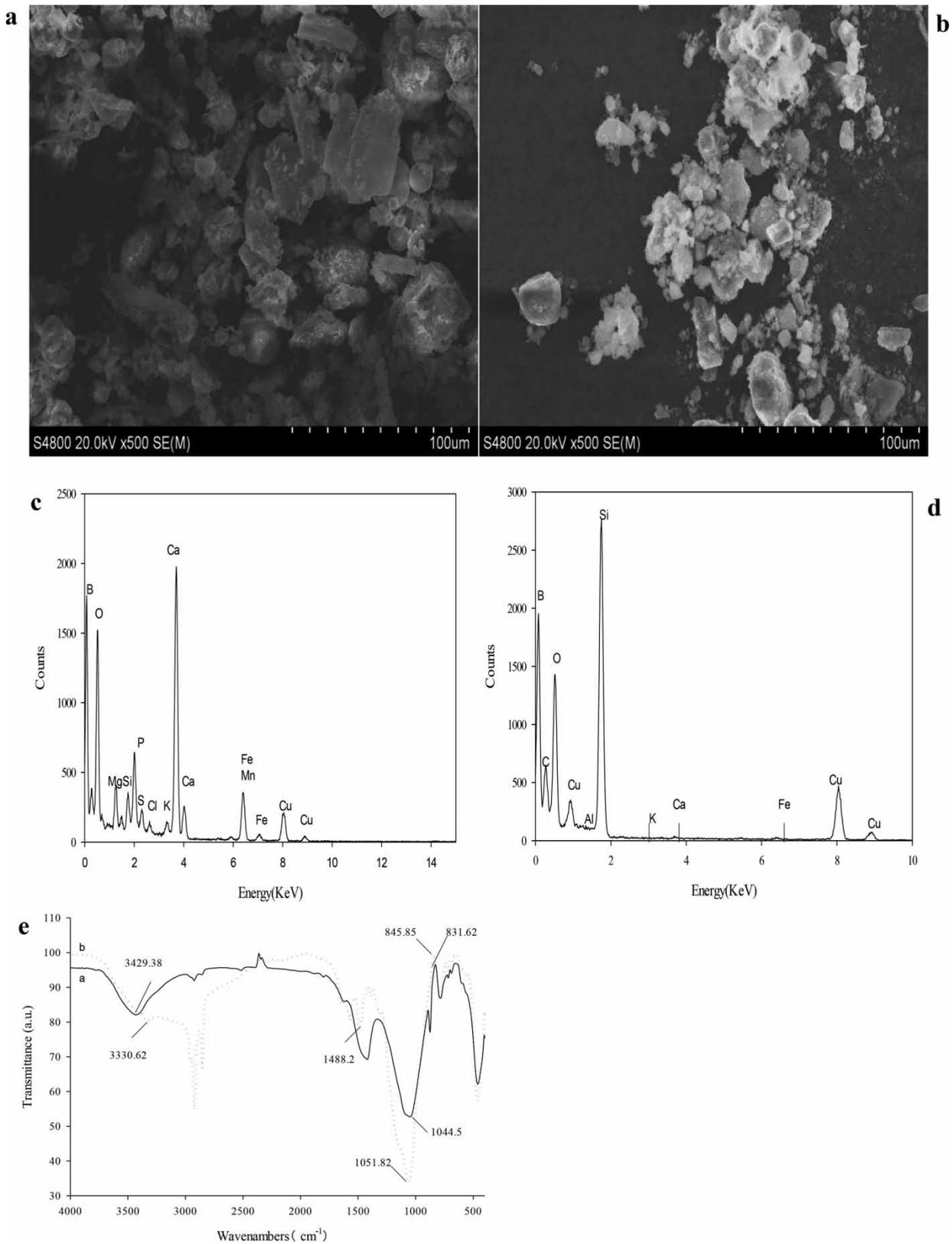
Figure 1 │ (a) SEM of biomass ash at 20 KeV; magnification 500. (b) SEM of synthesized matrix at 20 keV; magnification 500. (c) EDS analysis of elemental composition of biomass ash. (d) EDS analysis of elemental composition of modified biomass ash. (e) FTIR spectra: (a) biomass ash and (b) synthesized matrix.

Table 2 | Comparison of the BET analysis of functionalized HMS, biomass ash, and synthesized matrix

Analysis	Sample		
	HMS-NH2 (Machida *et al.* 2012)	Fly ash	Fly ash + HMS +10% APS
BET surface area (m² /g)	17	21.38 ± 0.17	185.81 ± 0.15
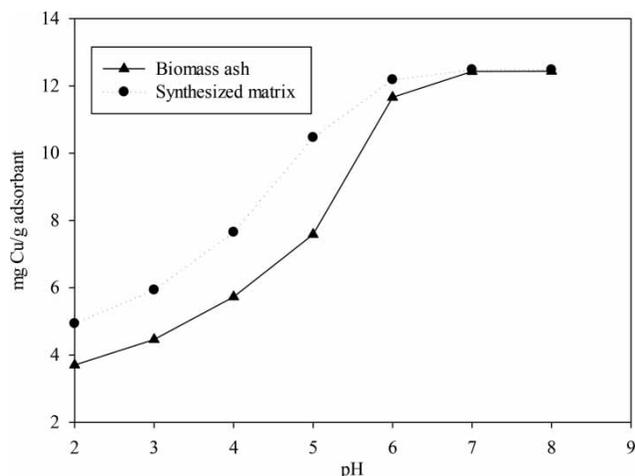
Figure 2 | Effect of pH on the adsorption of Cu²⁺ on biomass ash and modified biomass ash (initial concentrations of Cu²⁺, 50 mg/L; biomass ash concentration, 4 g/L; T = 30 °C).

exchange mechanism of H⁺ and metal ions in solution can be represented by the following equations:

$$XOH + H_3O^+ \rightarrow XOH_2 + H_2O \tag{1}$$

$$XOH + OH^- \rightarrow XO^- + H_2 \tag{2}$$

$$2(XO^-) + M^{2+} \rightarrow (XO)^2M \tag{3}$$
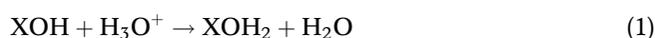
X: Si, Fe, and Al
M: metal

With the increase of pH, The negative charge on the surface of the material is improved, thus improving the electrostatic force between the adsorbent and adsorbate (Ren *et al.* 2011; Zarime *et al.* 2014). The maximum adsorption efficiency of Cu²⁺ on the biomass ash and modified material were observed between pH 5 and 6. When pH >6, the weak adsorption of Cu²⁺ can be attributed to the precipitation of Cu²⁺ species such as carbonates or

hydroxides (Figure 2), according to the distribution of metal species effected by pH (Kim *et al.* 2008).

The modified material was functionalized with NH₂ groups, thus forming an amino-Cu complex with a larger stability constant which can promote the formation of this compound. The stability of the compound mainly depends on the pH which must be near 7 (Walcarius & Mercier 2010; Awual *et al.* 2014). The adsorption mechanism of Cu²⁺ on the modified material was mainly dependent on the protonation of N. When pH was less than 3, a large amount of H⁺ was present in the solution, the functional groups on the adsorbent surface mainly bind H⁺ which made it difficult for Cu²⁺ to adsorb. The functional groups on the surface of the adsorbent existed in the form of Schiff bases (-N = CH-) when the solution pH was greater than 5, the H⁺ react with the lone pair of electrons of nitrogen, thereby preventing the combination of Cu²⁺ with NH₂ groups.

Adsorption isotherm of synthesized material

Table 3 lists a comparison of the Cu²⁺ adsorption capacity of several types of adsorbents reported when the pH of the solution is ~5, and the adsorption capacity of the modified biomass ash is better than most other materials. The BET analysis results showed that the specific surface area of the modified biomass ash was greatly improved, which explains the remarkable increase in the adsorption capacity for different initial Cu²⁺ concentrations. In addition, in order to

Table 3 | Comparison of Cu²⁺ adsorption capacities of different absorbents

Absorbent	Adsorption capacity (mg/g)	pH	Reference
Synthesized matrix	25.0	5	
Peanut shell	0.625	5	Shi *et al.* (2012)
Banana peel	22.8	5	Jasem (2015)
Biochar	8.85	5	Adeyemo *et al.* (2014)
Coal fly ash	20.9	5	Jasem (2015)
Bentonite	22.9	5.5	Fan *et al.* (2013)
Sepiolite	9.64	5	Dönmez *et al.* (2015)
Zeolite	23.0	6.5	Wang *et al.* (2008)
Activated carbon	43.3	6	Demiral & Güngör (2016)
Clays	3–11	5	O'Connell *et al.* (2008)

describe the characteristics of adsorption process, the Langmuir and Freundlich adsorption models were used to fit the results. The form of Langmuir equation can be expressed as follows (Langmuir 1918):

$$\frac{Ce}{qe} = \frac{1}{q_L \cdot K_L} + \frac{Ce}{q_L} \tag{4}$$

where Ce represents the equilibrium concentration of the metal ion (mg/L), q_e the amount of metal ions adsorbed by a unit mass adsorbent (mg/g), q_L represents the maximum amount of the metal ion adsorbed by the unit mass adsorbent (mg/g), and K_L represents the Langmuir constant (L/mg). The Langmuir isotherm is a monolayer model for adsorption, mainly applicable to the adsorption which occurs on the surface of the material. The Freundlich equation can be expressed as follows (Freundlich 1906):

$$\ln(q_e) = \ln(K_F) + \frac{1}{n} \ln(Ce) \tag{5}$$

where q_e and Ce are the same as defined above, K_F (mg/g) (mg/L)$^{1/n}$ and n are the Freundlich constants which can indicate the adsorption capacity and the adsorption strength of a given material, respectively.

The Freundlich isotherm is a multilayer model, applicable to nonideal sorption on heterogeneous surfaces. The parameters of the two models were obtained by fitting the experimental results. Table 4 shows the fitting results of the parameters of both the models at different temperatures. Both the adsorption models fitted with the experimental data obtained for biomass ash and the synthesized matrix (Table 4); however, the Langmuir model showed a better fit for biomass ash while the Freundlich model showed a better fit for the modified product. This was probably because the adsorption of Cu²⁺ by biomass ash belonged to monolayer adsorption T, thus the fitting of the experimental data was better at every temperature. However, the adsorption

of Cu²⁺ by the modified biomass ash belonged to multilayer adsorption. The functional groups on the surface of the adsorbent existed in the form of Schiff bases (-N = CH-), and the -N = CH- would complex with Cu²⁺ which lead to the reaction of Cu²⁺ on the surface of the material was not only the adsorption reaction but also complexation reaction. This might be the reason why the reaction did not fit to the Langmuir model. Moreover, the favorability of adsorption is also very important. In the Freundlich model, the constant $1/n$ indicates the adsorption intensity; the adsorption progress is a favorable adsorption when the n values is between 1 and 10 (Bourliva *et al.* 2013). In our study, the n values were greater than 3 at every temperature, indicating a favorable adsorption of Cu²⁺ onto the modified biomass ash (Table 4). The effect of temperature on adsorption showed that with the increase of temperature, the adsorption capacity got a small increase. The possible explanation is that the adsorption process is an endothermic reaction, and the temperature can increase the internal structure of the modified biomass ash (Al-Degs *et al.* 2008), and the adsorption capacity is enhanced.

Thermodynamic studies

The thermodynamic equation can be expressed as follows (Gupta & Ali 2004):

$$\Delta G^0 = -RT \ln K_L' \tag{6}$$

$$\ln \frac{KL2}{KL1} = -(\Delta H^0/R)\left(\frac{T1 - T2}{T2T1}\right) \tag{7}$$

$$\Delta S^0 = \frac{\Delta H0 - \Delta G0}{T} \tag{8}$$

where K_L', K_{L1}, and K_{L2} are the Langmuir constants at T, $T1$ and $T2$, respectively; R is gas constant, the value is 8.314

Table 4 │ Values of the constants and fitting of the adjusted adsorption models

Adsorbent	Temp (°C)	Langmuir			Freundlich		
		q_L (mg/g)	K_L (L/mg)	R^2	n	K_F (mg/g)(mg/L)$^{1/n}$	R^2
Biomass ash	30	19.82	1.58	0.998	8.23	13.86	0.909
	45	20.79	1.82	0.998	6.84	13.78	0.939
	60	21.74	2.09	0.996	5.79	13.57	0.909
Modified biomass ash	30	24.21	6.45	0.995	6.59	19.14	0.998
	45	24.45	8.35	0.996	6.61	19.99	0.998
	60	24.51	9.49	0.996	6.62	20.41	0.999

J·mol^{-1}·K^{-1}. From the view of thermodynamics, adsorption free energy ΔG is the adsorption driving force, reflects the strength of the driving force for adsorption, which depends on the size of the enthalpy and entropy factors. The negative value of ΔG and the positive value of ΔH and ΔS indicated that the entropy change was the main driving force in the process of adsorption (Table 5). Meanwhile, the negative value of ΔG indicated that Cu^{2+} tends to be adsorbed from solution to the modified biomass ash; in other words, the adsorption of Cu^{2+} on the material was favorable and spontaneous. With the increase of temperature, ΔG becomes smaller gradually, and the result showed that the rising temperature was propitious to the adsorption process. Adsorption can be divided into chemical adsorption and physical adsorption, but in one adsorption process, the two effects can occur simultaneously. Generally, physical adsorption force is less than the chemical adsorption force. Chen's research results showed that when the adsorption force was van Edward force, hydrogen bond, ligand exchange, dipole interaction and chemical bond, the adsorption heat was 4–10, 2–40, ≈40, 2–29 and >60 kJ·mol^{-1}, respectively (Jie *et al.* 2012). In our study, the $\Delta H > 0$, which indicated the adsorption process was endothermic process, the increase of temperature was beneficial to the adsorption process. At the same time, as shown in Table 5, the ΔH was 13.9, which can reveal that the adsorption force was hydrogen bond, ligand exchange; this also indicated that the adsorption process not only contains physical adsorption, but also chemical adsorption.

Kinetic adsorption studies

Figure 3 shows the adsorption kinetics of Cu^{2+} from solutions onto biomass ash and the modified product, residual concentration of Cu^{2+} vs sorption time was illustrated at 30 °C. Figure 3 indicates that the residual Cu^{2+}
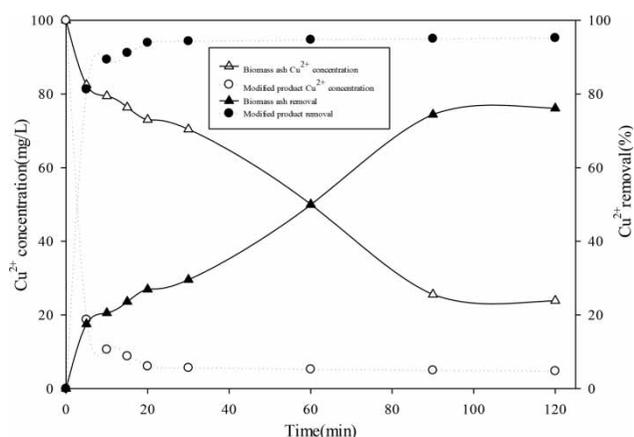
Table 5 │ Thermodynamic parameters for biomass ash and the synthesized matrix

	Temp. (°C)	Thermodynamic parameters		
		ΔG^0(kJ·mol^{-1})	ΔH^0(kJ·mol^{-1})	ΔS^0 (J·mol^{-1}·K^{-1})
Biomass ash	30	−1.16	7.60	28.7
	45	−1.55		
	60	−2.05		
Synthesized matrix	30	−4.71		
	45	−5.63	13.9	61.2
	60	−6.25		

Figure 3 │ Sorption kinetics: concentration and removal (%) of Cu^{2+} from aqueous solution vs. sorption time (initial concentrations of Cu^{2+}, 100 mg/L; biomass ash and modified product concentration, 2 g/L; T = 30 °C; initial pH 5.0).

concentration reduced sharply during the first 20–30 min and reached a value less than 10 mg/L within 120 min. For biomass ash, however, it took a much longer time to reach equilibrium and the Cu^{2+} concentration was about 5 times that of the modified product in equilibrium. At the initial stages of the reaction, when the active adsorption sites on the material surface were not occupied, the Cu^{2+} can be quickly absorbed onto the surface of the material (Sharma *et al.* 2017). However, with the adsorption process, the active adsorption sites on the surface of the material were more and more occupied by Cu^{2+} which led to the reduce of unoccupied available sites, thus the sorption rate also decreased rapidly (Ji *et al.* 2017). The slower diffusion of Cu^{2+} onto the interior matrix of the modified biomass ash may also lead to the slower adsorption rate at this stage (Motsi *et al.* 2009). In order to analyze the adsorption rate of Cu^{2+} on modified biomass ash, the results of the dynamic analysis were performed by the pseudo-first-order and pseudo-second-order rate equations (Mobasherpour *et al.* 2014; Nashtifan *et al.* 2017). The two models can be expressed as follows:

$$\ln(Q_e - Q_t) = \ln Q_e - k_1 t \tag{9}$$

$$\frac{t}{Q_t} = \frac{1}{k_2 Q_e^2} + \frac{t}{Q_e} \tag{10}$$

where Q_e is the adsorption capacity (mg·g^{-1}) at equilibrium, Q_t is the amount (mg·g^{-1}) of material adsorbed at time t, k_1 represents the rate constant (min^{-1}) of the pseudo-first-order model, and k_2 is the rate constant (g·mg^{-1}·min^{-1}) of pseudo-second-order model. Table 6 shows the kinetic parameters

Table 6 | Kinetic parameters for biomass ash and the synthesized matrix

Adsorbent	Temp. (°C)	Pseudo-first-order model		Pseudo-second-order model	
		k_1 (min^{-1})	R^2	k_2 (g·mg^{-1}·min^{-1})	R^2
Biomass ash	30	2.75×10^{-2}	0.943	1.25×10^{-3}	0.824
Synthesized matrix		2.23×10^{-2}	0.496	8.17×10^{-2}	1

of the adsorption for Cu²⁺ on the two materials at 30 °C. The values of R^2 was larger than that obtained using the pseudo-second-order model for biomass ash, but the result was quite the opposite for the modified biomass ash. This result also indicated that the adsorption of the modified biomass ash for Cu²⁺ was mainly chemical adsorption. This chemical adsorption process may be caused by the reaction force and the coordination process between the Cu²⁺ and -NH₂, -NH- on the surface of the modified material.

CONCLUSIONS

This new material synthesized from biomass ash shows a better adsorption capacity for Cu²⁺ and the capacity mainly depends on the initial metal concentration and the initial pH. Compared to the untreated biomass ash, the modified material shows a much larger specific surface area and a greater number of active adsorption sites because of the functionalization of the mesoporous material with APS. The adsorptions of Cu²⁺ on the modified biomass ash fit the Freundlich well. The adsorption processes is endothermic and follows pseudo-second-order kinetics. Notably, this new material has shown a strong adsorption capacity compared to the reported materials. This study provides a good method for the utilization of biomass ash in the environment.

ACKNOWLEDGEMENTS

REFERENCES

Adeyemo, A., Adebowale, K. & Olu-Owolabi, B. 2014 Adsorption of copper by biochar. *International Research Journal of Pure and Applied Chemistry* **4**, 727–735.

Al-Degs, Y. S., El-Barghouthi, M. I., El-Sheikh, A. H. & Walker, G. M. 2008 Effect of solution pH, ionic strength, and temperature on adsorption behavior of reactive dyes on activated carbon. *Dyes and Pigments* **77**, 16–23.

Ali, R. M., Hamad, H. A., Hussein, M. M. & Malash, G. F. 2016 Potential of using green adsorbent of heavy metal removal from aqueous solutions: adsorption kinetics, isotherm, thermodynamic, mechanism and economic analysis. *Ecological Engineering* **91**, 317–332.

Alyoshina, N. A. & Parfenyuk, E. V. 2013 Functionalized mesoporous silica materials for molsidomine adsorption: thermodynamic study. *Journal of Solid State Chemistry* **205**, 211–216.

Awual, M. R., Hasan, M. M. & Shahat, A. 2014 Functionalized novel mesoporous adsorbent for selective lead(II) ions monitoring and removal from wastewater. *Sensors & Actuators B Chemical* **203**, 854–863.

Boukai, A. I., Bunimovich, Y., Tahir-Kheli, J., Yu, J. K. & Heath, J. R. 2008 Silicon nanowires as efficient thermoelectric materials. *Nature* **451**, 168–171.

Bourliva, A., Michailidis, K., Sikalidis, C., Filippidis, A. & Betsiou, M. 2013 Lead removal from aqueous solutions by natural Greek bentonites. *Clay Minerals* **48**, 771–787.

Cao, M., Sheng, Z. & Zhang, H. 2016 Effect of pH value on graphene-containing composite materials for heavy metal ions adsorption. *Journal of Functional Materials* **9**, 9051–9056.

Ciesielczuk, T., Rosikdulewska, C. & Kochanowska, K. 2014 The influence of biomass ash on the migration of heavy metals in the flooded soil profile – model experiment. *Archives of Environmental Protection* **40**, 3–15.

Cretescu, I., Soreanu, G. & Harja, M. 2015 A low-cost sorbent for removal of copper ions from wastewaters based on sawdust/fly ash mixture. *International Journal of Environmental Science and Technology* **12**, 1799–1810.

Demiral, H. & Güngör, C. 2016 Adsorption of copper(II) from aqueous solutions on activated carbon prepared from grape bagasse. *Journal of Cleaner Production* **124**, 103–113.

Dönmez, M., Camcı, S., Akbal, F. & Yağan, M. 2015 Adsorption of copper from aqueous solution onto natural sepiolite: equilibrium, kinetics, thermodynamics, and regeneration studies. *Desalination & Water Treatment* **54**, 2868–2882.

Fan, H., Pan, Z., Zhang, H., Gong, J., Hu, G., Wei, Z. & Xiao, C. 2013 Adsorption for BTA and Cu with bentonite. *Industrial Water Treatment* **33**, 38–41.

Freundlich, H. 1906 Over the adsorption in solution. *Journal of Physical Chemistry* **57**, e470.

Gupta, S. S. & Bhattacharyya, K. G. 2008 Immobilization of Pb (II), Cd (II) and Ni (II) ions on kaolinite and montmorillonite surfaces from aqueous medium. *Journal of Environmental Management* 87, 46–58.

Gupta, V. K. & Ali, I. 2004 Removal of lead and chromium from wastewater using bagasse fly ash – a sugar industry waste. *Journal of Colloid and Interface Science* 271, 321–328.

Hao, S., Verlotta, A., Aprea, P., Pepe, F., Caputo, D. & Zhu, W. 2016 Optimal synthesis of amino-functionalized mesoporous silicas for the adsorption of heavy metal ions. *Microporous & Mesoporous Materials* 236, 250–259.

Hu, H., Jin, Q. & Kavan, P. 2014 A study of heavy metal pollution in China: current status, pollution-control policies and countermeasures. *Sustainability* 6, 5820–5838.

James, A. K., Thring, R. W., Helle, S. & Ghuman, H. S. 2012 Ash management review-applications of biomass bottom ash. *Energies* 5, 3856–3873.

Jasem, L. N. A. 2015 Removal of copper (II) and cadmium (II) ions from aqueous solutions using banana peels and bentonite clay as adsorbents. *Journal of Engineering and Development* 19, 1873–1822.

Ji, X. D., Ma, Y. Y., Peng, S. H., Gong, Y. Y. & Zhang, F. 2017 Simultaneous removal of aqueous Zn^{2+}, Cu^{2+}, Cd^{2+}, and Pb^{2+} by zeolites synthesized from low-calcium and high-calcium fly ash. *Water Science & Technology* 76 (8), 2106–2119.

Jiang, S., Huang, L., Nguyen, T. A., Ok, Y. S., Rudolph, V., Yang, H. & Zhang, D. 2016 Copper and zinc adsorption by softwood and hardwood biochars under elevated sulphate-induced salinity and acidic pH conditions. *Chemosphere* 142, 64–71.

Jie, F., Yanhu, L. & Changcan, Y. 2012 Study on the adsoption kinetics and thermodynamics of DMF on macroporous adsorbents. *Acta Scientiae Circumstantiae* 32, 639–644.

Kim, D. H., Shin, M. C., Choi, H. D., Seo, C. I. & Baek, K. 2008 Removal mechanisms of copper using steel-making slag: adsorption and precipitation. *Desalination* 223, 283–289.

Krawiec, P. & Kaskel, S. 2006 Thermal stability of high surface area silicon carbide materials. *Journal of Solid State Chemistry* 179, 2281–2289.

Langmuir, I. 1918 The adsorption of gases on plane surfaces of glass, mica and platinum. *Journal of the American Chemical Society* 40, 1361–1403.

Liu, W., Xu, N., Wang, T., Xiong, L. & Ni, J. 2013 Influence of pH, ionic strength and humic acid on competitive adsorption of Pb(II), Cd(II) and Cr(III) onto titanate nanotubes. *Chemical Engineering Journal* 215, 366–374.

Machida, M., Fotoohi, B., Amamo, Y., Ohba, T., Kanoh, H. & Mercier, L. 2012 Cadmium (II) adsorption using functional mesoporous silica and activated carbon. *Journal of Hazardous Materials* 221, 220–227.

Madani, N., Bouchenafa-Saib, N., Mohammedi, O., Varela-Gandía, F. J., Cazorla-Amorós, D., Hamada, B. & Cherifi, O. 2017 Removal of heavy metal ions by adsorption onto activated carbon prepared from Stipa tenacissima leaves. *Desalination & Water Treatment* 64, 179–188.

Mendicino, L. & Brown, P. T. 1998 The environment, health and safety side of copper metalization. *Semiconductor International* 6, 105–110.

Messina, P. V. & Schulz, P. C. 2006 Adsorption of reactive dyes on titania-silica mesoporous materials. *Journal of Colloid & Interface Science* 299, 305–320.

Mobasherpour, I., Salahi, E. & Ebrahimi, M. 2014 Thermodynamics and kinetics of adsorption of Cu(II) from aqueous solutions onto multi-walled carbon nanotubes. *Journal of Saudi Chemical Society* 18, 792–801.

Motsi, T., Rowson, N. & Simmons, M. 2009 Adsorption of heavy metals from acid mine drainage by natural zeolite. *International Journal of Mineral Processing* 92, 42–48.

Nashtifan, S. G., Azadmehr, A. & Maghsoudi, A. 2017 Comparative and competitive adsorptive removal of Ni^{2+} and Cu^{2+} from aqueous solution using iron oxide-vermiculite composite. *Applied Clay Science* 140, 38–49.

Ndilila, W., Callan, A. C., McGregor, L. A., Kalin, R. M. & Hinwood, A. L. 2014 Environmental and toenail metals concentrations in copper mining and non mining communities in Zambia. *International Journal of Hygiene & Environmental Health* 217, 62–69.

Noli, F., Buema, G., Misaelides, P. & Harja, M. 2015 New materials synthesized from ash under moderate conditions for removal of toxic and radioactive metals. *Journal of Radioanalytical and Nuclear Chemistry* 303, 2303–2311.

O'Connell, D. W., Birkinshaw, C. & O'Dwyer, T. F. 2008 Heavy metal adsorbents prepared from the modification of cellulose: a review. *Bioresource Technology* 99, 6709–6724.

Okmanis, M., Lazdiņa, D. & Lazdiņš, A. 2015 The composition and use value of tree biomass ash. *Rural Sustainability Research* 34, 32–37.

Pizarro, J., Castillo, X., Jara, S., Ortiz, C., Navarro, P., Cid, H., Rioseco, H., Barros, D. & Belzile, N. 2015 Adsorption of Cu^{2+} on coal fly ash modified with functionalized mesoporous silica. *Fuel* 156, 96–102.

Qiang, L. I., Liu, Y. N., Dong-Kai, L. I., Wang, H. & Xie, Y. C. 2015 Absorption study of Cu^{2+} on the peanut shell activated carbon. *Guangzhou Chemical Industry* 13, 76–78.

Quirantes, M., Calvo, F., Romero, E. & Nogales, R. 2016 Soil-nutrient availability affected by different biomass-ash applications. *Journal of Soil Science & Plant Nutrition* 16, 159–163.

Ren, X., Chen, C., Nagatsu, M. & Wang, X. 2011 Carbon nanotubes as adsorbents in environmental pollution management: a review. *Chemical Engineering Journal* 170, 395–410.

Saeung, S. & Boonamnuayvitaya, V. 2008 Adsorption of formaldehyde vapor by amine-functionalized mesoporous silica materials. *Journal of Environmental Sciences (China)* 20, 379–384.

Seweryn, A. 2012 The identification of the sorption properties of ash from arboreal biomass used to remove biogenic compounds and heavy metal ions from polluted water. *Genome* 45, 1077–1082.

Sharma, R., Sarswat, A., Pittman, C. U. & Mohan, D. 2017 Cadmium and lead remediation using magnetic and non-magnetic sustainable biosorbents derived from *Bauhinia purpurea* pods. *RSC Advances* 7, 8606–8624.

Shen, X., Qiu, G., Yue, C., Min, G. & Mei, Z. 2017 Multiple copper adsorption and regeneration by zeolite 4A synthesized from

bauxite tailings. *Environmental Science & Pollution Research International* **27**, 21829–21835.

Shi, W., Yan, S. & Tang, D. 2012 Adsorption of copper (II) on modified peanut shells. *Lizi Jiaohuan Yu Xifu/ion Exchange & Adsorption* **28**, 442–448.

Sočo, E. & Kalembkiewicz, J. 2013 Adsorption of nickel(II) and copper(II) ions from aqueous solution by coal fly ash. *Journal of Environmental Chemical Engineering* **1**, 581–588.

Takaishi, M., Osima, H. & Asano, S. 2015 Pollution caused by Ashio Copper Mine and its effects on environment and human health. *International University of Health and Welfare* **20**, 18603–18609.

Tamayo, A., Mazo, M. A., Ruiz-Caro, R., Martín-Illana, A., Bedoya, L. M., Veiga-Ochoa, M. D. & Rubio, J. 2015 Mesoporous silicon oxycarbide materials for controlled drug delivery systems. *Chemical Engineering Journal* **280**, 165–174.

Vamvuka, D. & Kakaras, E. 2011 Ash properties and environmental impact of various biomass and coal fuels and their blends. *Fuel Processing Technology* **92**, 570–581.

Walcarius, A. & Mercier, L. 2010 Mesoporous organosilica adsorbents: nanoengineered materials for removal of organic and inorganic pollutants. *Journal of Materials Chemistry* **20**, 4478–4511.

Wang, S., Terdkiatburana, T. & Tad Eacute, M. O. 2008 Adsorption of Cu(II), Pb(II) and humic acid on natural zeolite tuff in single and binary systems. *Separation & Purification Technology* **62**, 64–70.

Wang, Y. J., Liu, C., Zhou, D. M. & Chen, H. M. 2014 A critical view on the status quo of the farmland soil environmental quality in China: discussion and suggestion of relevant issues on report on the national general survey of soil contamination. *Journal of Agro-Environment Science* **8**, 1465–1473.

Williams, T. M. 1997 Obtaining water quality permits for land application of biomass boiler ash. *Biomass & Bioenergy* **13**, 279–287.

Xia, Y. & Mokaya, R. 2003 Highly ordered mesoporous silicon oxynitride materials as base catalysts. *Angewandte Chemie* **42**, 2639–2644.

Zarime, N. A., Wan, Z. Y. & Krishna, L. S. 2014 Adsorption of nickel and zinc by residual soils. *American Journal of Environmental Sciences* **10**, 523–529.

Zhang, H., Yang, J., Wu, J. & Lu, X. 2013 Study on treatment of electroplate wastewater with copper by ion-exchange and electrodeposition. *Technology of Water Treatment* **39**, 94–95.

Zhu, W., Wang, J., Wu, D., Li, X., Luo, Y., Han, C., Ma, W. & He, S. 2017 Investigating the heavy metal adsorption of mesoporous silica materials prepared by microwave synthesis. *Nanoscale Research Letters* **12**, 323–331.